

## SECTION VIII TWO-DIMENSIONAL HYDRODYNAMICS

### ON THE HYDRODYNAMICS OF SOAP FILMS

Y. COUDER<sup>a</sup>, J.M. CHOMAZ<sup>b</sup> and M. RABAUD<sup>a</sup>

<sup>a</sup>Groupe de Physique des Solides de l'Ecole Normale Supérieure, 24 rue Lhomond, 75231 Paris Cedex 05, France

<sup>b</sup>Centre National de Recherches Météorologiques, 42 Avenue G. Coriolis, 31057 Toulouse Cedex, France

Several experiments aiming at the exploration of the hydrodynamical properties of soap films are presented. Their interpretation takes into account the very specific equation of state of these films. It is shown that on short time scales each element of the film moves as a whole so that the film can be considered as a two-dimensional fluid with a local density proportional to its thickness.

When set horizontally, quasi two-dimensional turbulent flows can be obtained. The film behaves as an incompressible fluid whenever the motions occur at velocities small compared to the velocity of its elastic waves. An estimate of the role of air friction is given.

The static quasi equilibrium of a film when set vertical is discussed. Phenomena equivalent to the rise of buoyant bubbles can be obtained. It is shown that lee waves can also be generated confirming that a vertical soap film has the dynamical properties of a two-dimensional density stratified fluid.

#### 1. Introduction

Specific properties of soap films such as their stability, their elasticity, their topology when stretched on various frames, etc., have been investigated since a long time. Early studies are due to Plateau [1] and Gibbs [2]. A book by Boys [3] describes several remarkable experiments demonstrating the properties of capillary forces. More recent extensive articles on soap films are due to Mysels et al. [4] and to Rusanov and Krotov [5].

Our viewpoint in the present article will be different; we dispose with soap films of very thin, self-sustained, fluid layers in which classical hydrodynamical experiments can be done. In this medium the velocity field is confined to a surface and is practically two-dimensional. But soap films are complex objects; it is our aim here to discuss their hydrodynamical properties as they can be built up from their very specific physics. We will briefly recall, to illustrate these properties, several experiments [6–12] that we performed previously,

and we will present a few new ones. Experiments by Gharib and Derango [13] to be published in the present issue confirm the promises of the study of the hydrodynamics of soap films regarding the investigation of two-dimensional turbulent flows.

#### 2. Physical properties of soap films

##### 2.1. *Solutions of surfactants*

Soap molecules are usually formed of a hydrophilic polar head with a hydrophobic hydrocarbon tail. This association gives these molecules their properties as surfactants. When dissolved in water, they tend to settle at the free surface so that their hydrophobic part avoids the contact with water. Common soaps are made of a mixture of several surfactants, and the water used is not pure so that the real situation is complicated. However, the general features of soap films properties can

be understood in a model system. We will here consider a standard solution of only one type of soap molecule, with an initial concentration  $c_0$ , in pure water. Quantitative data will be taken from Rusanov and Krotov [5] and correspond to solutions of Sodium Dodecyl Sulfate (S.D.S.).

When a solution is set in a vessel, at equilibrium, there is a concentration  $\Gamma_1$  of soap molecules at the free surface and a concentration  $c_1$  in the bulk of the fluid. The values of  $\Gamma_1$  and  $c_1$  are determined by the equality of the chemical potentials of the molecules at the surface and in the bulk.

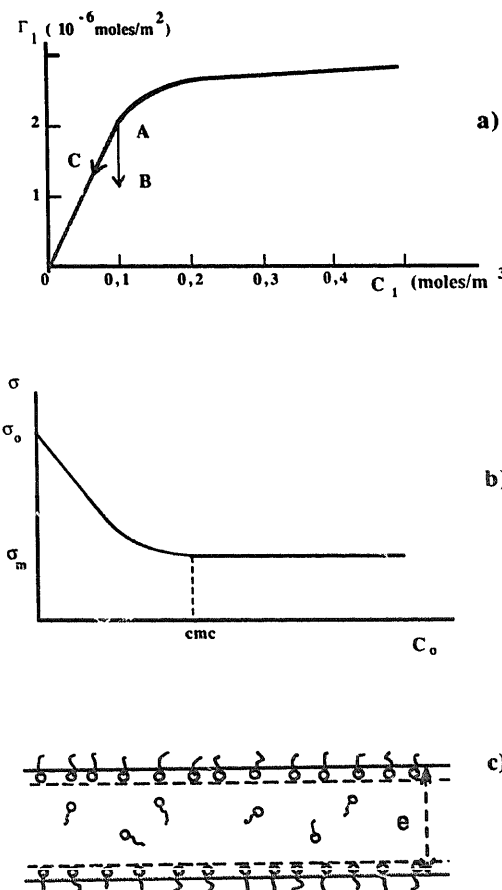


Fig. 1. (a) The surface concentration  $\Gamma_1$  of soap molecules adsorbed at the interface as a function of the volumic concentration  $c_1$  in the bulk of the fluid (adsorption isotherms). (From Rusanov and Krotov [5], p. 460.) The segments AB and AC represent respectively a Marangoni and a Gibbs stretching of the film. (b) The isothermal dependence of the surface tension  $\sigma$  on the concentration  $c_0$  of the solution. (c) Cross section of a thick soap film.

Fig. 1(a) gives a typical relation between the values of  $\Gamma_1$  and  $c_1$ . Two ranges of soap concentrations must be considered separately:

i) Small concentrations: The relation between  $\Gamma_1$  and  $c_1$  is linear, and we can write

$$\Gamma_1 = kc_1. \quad (1)$$

For a standard surfactant as S.D.S.,  $k$  is of the order of  $4 \mu\text{m}$ , showing that, in these states, the surface concentration is much larger than the volumic one. Typically, at the free surface the mean area per soap molecule is  $1.5 \text{ nm}^2$ , while in the bulk the mean volume per molecule is  $3 \times 10^4 \text{ nm}^3$ . A limit case is that of insoluble surfactants for which  $k = \infty$ , so that  $\Gamma_1 \neq 0$  while  $c_1 = 0$ .

For both soluble and insoluble surfactants, at low concentrations, the equation of state of the molecules at the surface can be approximated by a perfect gas law.

ii) Large concentrations: the relation between  $\Gamma_1$  and  $c_1$  is no longer linear and there is a sharp bend in the characteristics where  $\Gamma_1$  practically saturates. It occurs at a value of  $c_1$  called the critical micelles concentration (c.m.c.) because at this value, in the bulk, the molecules start forming clusters (called micelles) in which their hydrophobic tail is isolated from the water.

Generally, for a given solution of concentration  $c_0$ , the equilibrium values  $\Gamma_1$  and  $c_1$  will depend upon the shape of the container. In a usual vessel the free surface is very small so that the total quantity of soap at the surface is negligible, and  $c_1$  is equal to  $c_0$  (except for very small concentrations). This is no longer the case if the soap solution is set in a thin layer where the ratio of the area to the volume becomes large. In soap films, which have two water-air interfaces and a thickness of the order of a micrometer, we will always have to take into account the equilibrium between  $\Gamma_1$  and  $c_1$ .

## 2.2. Surface tension

At a given temperature, the surface tension of the interface,  $\sigma$ , is usually given as a function of

the solution concentration  $c_0$  (for a bulk fluid  $c_0$  is equal to  $c_1$ ) (fig. 1(b)). For small concentrations  $\sigma$  decreases linearly with  $c_0$ . At concentrations larger than the critical micelle concentration, the decrease of  $\sigma$  with  $c_0$  becomes very slow. The dependence is written

$$\sigma = \sigma_0 - f, \quad (2)$$

where  $\sigma_0$  is the surface tension of pure water and  $f$  is called the spreading pressure (of surface pressure) of the surfactant. More generally in a given object (solution, film, ...),  $f$  is related to the surface and interstitial concentrations ( $\Gamma_1$  and  $c_1$ ) by the Gibbs adsorption law:

$$df = RT\Gamma_1 d(\ln \gamma_1 c_1),$$

where  $R$  is the gas constant and  $\gamma_1$  is an activity coefficient.

– In the small concentration range, the activity coefficient is  $\gamma_1 = 1$  and the relation (1) is valid so that the Gibbs law can be integrated. The equation of state of the soap molecules at the interface is then a two-dimensional perfect gas law:

$$f = RT\Gamma_1, \quad (3)$$

where  $R$  is the gas constant.

– For large concentrations, the situation is more complicated:  $\gamma_1$  deviates from unity and the adsorbed concentration  $\Gamma_1$  increases only very slowly with  $c_1$ . The evolution of  $f$  is then usually described by a Szyszkowski–Langmuir equation [16]

$$f = RT\Gamma_\infty \ln\left(1 + \frac{c_1}{a_1}\right), \quad (4)$$

where  $\Gamma_\infty$  and  $a_1$  are empirical constants chosen for a given soap to fit the observed concentration dependence of  $f$ .

### 2.3. Films thickness

Before discussing their stability, we must recall the two characteristic states in which soap films are observed to exist. The usual soap bubbles,

observed in white light, show bright interference colors. Their thickness ranges from 0.1 to 10  $\mu\text{m}$ . We will call them thick films. They are formed (fig. 1(c)) of two superficial layers with a surface density of soap  $\Gamma_1$  separated by unorganized interstitial fluid of a soap solution of concentration  $c_1$ . In thick films there is no direct interaction between the two surface layers so that the film thickness can have any value. These films are not stable in the gravity field and we will discuss their drainage in section 3.

After drainage some films reach a state where, owing to their very small thickness, they hardly reflect light. They are called black films and can be in two states; the common black film has a thickness of the order of 30 nm, the second black film (Newton's black film) is only 4.5 nm thick. In thin films the two surface layers are also separated by some interstitial fluid but the strong interaction between the two surface layers determines the film's thickness. The potential of the interaction has a double well so that two thicknesses are observed. These films are in a metastable state; they can burst but cannot undergo further drainage, they cannot become thicker again either.

### 2.4. Formation, stability and elasticity of soap films

A film is usually formed by dipping a frame in a soap solution of concentration  $c_0$ . The stretching of the film on the frame is rapid and we can consider that the molecules do not have time to diffuse from one region of the film plane to another. The global concentration of soap in all regions of the film is the same and equal to  $c_0$ , and

$$c_0 = c_1 + 2\Gamma_1/e, \quad (5)$$

where  $c_1$  is the concentration of the interstitial fluid,  $\Gamma_1$  the concentration on each interface and  $e$  the film thickness. (The validity of this hypothesis which is an essential ingredient of the following analysis is not obvious, see note added in proof.)

The relative stability of soap films is due to their elasticity. We will consider a film with an equilibrium state represented on fig. 1(a) by the point A ( $\Gamma_1, c_1$ ). A local stretching disturbs the equilibrium between  $\Gamma_1$  and  $c_1$ .

– If the disturbance occurs on a short time scale, the soap molecules do not have time to diffuse out from the inner fluid to the surface, so that same number of molecules initially present at the interface are now scattered on a larger area. The state of the stretched film is represented by point B. The decrease of  $\Gamma_1$  results in an increase of the surface tension which opposes the stretching. This process is called the Marangoni elasticity and explains the film stability to rapid disturbances.

– If the time scale of the film stretching is longer, the molecules of the interstitial fluid have time to diffuse out to the surface. At each time there is a thermodynamic equilibrium between  $\Gamma_1$  and  $c_1$ . The stretching will displace the state of the film on fig. 1(a) from A to C. The resulting increase of the surface tension corresponds now to the Gibbs elasticity of the film.

Since the original work of Gibbs [2] the elasticity of soap films has been widely investigated [5, 14–16] and we will summarize here the results in the simplest cases.

The elasticity modulus of a film is defined by

$$E = 2 d\sigma/d(\ln A), \quad (6)$$

where  $A$  is the surface of the film. Due to relation (2) and since the fluid is incompressible, equivalent definitions are

$$E = -2A \frac{df}{dA} = -2e \frac{d\sigma}{de}. \quad (7)$$

In principle, the limit between the Marangoni and the Gibbs elasticity is given by the time scale  $\tau_D = e^2/D$  which characterizes the diffusive motion of soap molecules through the film thickness. As the diffusion coefficient  $D = 4 \times 10^{-6} \text{ cm}^2/\text{s}$ , for films  $1 \mu\text{m}$  thick  $\tau_D$  is of the order of 0.01 s. However, Rusanov and Krotov [5] argue that the

presence of impurities makes the equilibrium more difficult to reach so that Marangoni elasticity can be observed up to times of the order of a second.

The values of the elasticities can be deduced in each of the concentration ranges defined in section 2.1:

i) For small concentrations the Marangoni elasticity is

$$E_M = 2f = 2RT\Gamma_1, \quad (8)$$

where  $\Gamma_1$  can be deduced from (1) and (5):

$$\Gamma_1 = c_0 \frac{ek}{e + 2k}. \quad (9)$$

The Gibbs elasticity  $E_G$  can also be calculated:

$$E_G = -2e \frac{d\sigma}{de} = 4RTc_0 \frac{ek^2}{(e + 2k)^2}. \quad (10)$$

It is related to  $E_M$  by

$$E_G = \frac{2E_M k}{e + 2k}. \quad (11)$$

In the limit of thin films ( $e \ll 2k$ ),  $E_G \approx E_M$  because the interstitial fluid is too thin to provide soap molecules to the surface.

ii) For large concentrations of soap the relation (1) is no longer valid and relation (4) replaces relation (3) so that the expression of the Gibbs elasticity becomes more complex.

For simplicity, in the following, we will limit ourselves to small concentrations. It will be useful to remember that, typically, for a  $2 \mu\text{m}$  thick film of a dilute solution of S.D.S., the Gibbs elasticity is  $E_G = 30 \times 10^{-3} \text{ N/m}$ .

## 2.5. Waves propagation in films

G.I. Taylor [17] investigated the propagation of the waves in thin plane jets of pure water. In the most easily excited mode, the sinusoidal transverse motions of the two surfaces are in phase with each other (fig. 2(a)). For these waves (called antisym-

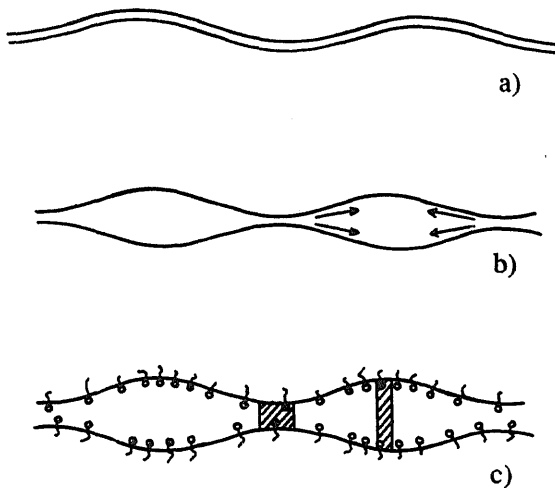


Fig. 2. Waves in a liquid film. (a) Antisymmetrical mode. (b) Symmetrical mode. (c) Elastic mode.

metrical waves by Taylor) the restoring force is due to surface tension and their velocity is

$$v_{AS} = \sqrt{\frac{2\sigma}{\rho e}}, \quad (12)$$

where  $\rho$  is the density of water.

The second mode that Taylor called symmetrical is a peristaltic mode where both surfaces move with opposite phases (fig. 2(b)). This mode, which involves viscous motion of the fluid from the nodes to the antinodes, is dispersive and propagates at

$$v_s = k_0 \sqrt{\frac{\sigma e}{2\rho}}, \quad (13)$$

where  $k_0$  is the wave vector.

In a soap film the propagation of the antisymmetrical mode is easily observed. A correction however must be applied; as the thickness of the film is very small, the surface density of the displaced fluid must be corrected to take into account the air motion. The thickness of the column of air set into motion by the vibration of the film is of the order of magnitude of the wavelength so that the effective surface density is given by

$$(\rho e)_{eff} = \rho e + 2\pi p_{air}/k_0, \quad (14)$$

where  $p_{air}$  is the density of air and  $k_0$  the wave vector.

The propagation of waves in soap film has been investigated by Lucassen et al. [18]. The motion of a peristaltic mode involves two possible processes of change in the local film thickness. The first one  $(\partial e/\partial t)_f$  is due to the internal viscous flows from one region to the other related, as in films of pure water, to variations of the Laplace pressure (fig. 2(b)). In the second one, the changes  $(\partial e/\partial t)_S$  is due to the elastic stretching of the surface films in the antinodes (fig. 2(c)). It can be shown [5] that the order of magnitude of the ratio of these two effects is

$$\left( \frac{\partial e}{\partial t} \right)_f / \left( \frac{\partial e}{\partial t} \right)_S \approx \frac{e^2 k_0^2}{4\pi^2} \ll 1, \quad (15)$$

where  $2\pi/k_0$  is the wavelength. As a result, in the soap films, the pure Taylor symmetrical mode can be neglected, and the waves are the elastic waves investigated by Lucassen et al. [18] where the variation of thickness are related to variation of the surface density of the surfactant molecules (fig. 2(c)). These waves propagate at a velocity

$$v_{LF} = \sqrt{\frac{2E}{\rho e}}. \quad (16)$$

Using a Marangoni elasticity  $E_M = 2f \approx 80 \times 10^{-3}$  N/m we find  $v_{LF} = 4$  m/s in a 10  $\mu\text{m}$  thick film, and  $v_{LF} \approx 13$  m/s in a film 1  $\mu\text{m}$  thick.

### 3. The near hydrostatic equilibrium of a vertical soap film

When a soap film, stretched on a rectangular frame, is set vertical it first shows a turbulent motion as its zone of unequal thickness are advected by their weight upwards or downwards. After a characteristic time  $\tau_1$  ( $\tau_1 \approx 10$  s) this violent motion stops and, when lit with monochromatic light, the film shows a pattern of horizontal interference fringes corresponding to a wedge-like

thickness. At this stage, in a 30 cm high frame, the thickness will vary typically from 0.2  $\mu\text{m}$  at the top of the frame to 10  $\mu\text{m}$  at the bottom. The observed fringes are not stationary; they move slowly downwards as the film thins down.

### 3.1. The thinning

The thinning of soap films has been investigated in details by Mysels et al. [4]. They showed that several processes could be observed, depending upon the state of the surface layers. We are only concerned here by their mobile films where the surface layers have a fluid behavior. In this case they observed that the thinning velocity depended mainly on the width of the frame. They showed that this rather surprising result is due to the general convective motion of the film created by *marginal regeneration*.

#### 3.1.1. Marginal regeneration

This process is linked with the existence between the film and the frame of a meniscus called the Plateau border. Inside this meniscus, because it is concave outwards, the capillary Laplace pressure is negative; it exerts a suction on the film nearby and creates zones of reduced thickness. For reasons discussed below, these zones are buoyant and move towards the top of the frame, pushing down the rest of the film. This convection has no threshold on the vertical part of the frame, so vertical borders are the active zones; the narrower the frame, the faster the thinning.

#### 3.1.2. Viscous thinning

If we consider now a film without a vertical frame (e.g. a spherical bubble or a film stretched between two horizontal circular rings), the observed thinning is slower by three orders of magnitude. There is no more global displacement of different zones of the film and the remaining thinning can be ascribed to the viscous flow of the inner fluid between motionless surfaces. The only acting forces are gravity, surface tension, and viscous friction (now the classical pressure in the

film is everywhere equal to the atmospheric pressure). For a stationary viscous flow between motionless parallel interfaces, the velocity profile is parabolic (Poiseuille flow). For a film 1  $\mu\text{m}$  thick, the maximum vertical velocity is then  $w \sim 2 \mu\text{m/s}$ .

In the two surface layers a vertical gradient of surface tension opposes the viscous stress exerted by the inner fluid:

$$\frac{d\sigma}{dz} = \mu \left( \frac{\partial w}{\partial x} \right)_{x=e/2} = g\rho e(z)/2. \quad (17)$$

This later equation means that the gradient of surface tension in the superficial layers carry the inner parts of the film. It could have been established more simply by neglecting altogether the Poiseuille flow and writing that the surface tension gradient balances the weight of an element of the film. There is then a strong analogy with the static equilibrium of a classical fluid. It is made more evident if we write eq. (17) using the spreading pressure defined by eq. (2):

$$2 \frac{df}{dz} = -g\rho e(z). \quad (18)$$

This is the equation of the equilibrium of a two-dimensional fluid where  $\rho e(z)$  is the surface density and  $2(df/dz)$  is the gradient of a two-dimensional hydrostatic pressure.

### 3.2. Thickness profiles

The film behaves as a compressible medium; its isothermal compressibility is the inverse of its elasticity. To seek its possible thickness profiles, we use the equation of state of the fluid. We will consider a film which, if it was perfectly horizontal, would have a constant thickness  $e^*$  and a constant tension  $\sigma^*$ , and seek its equilibrium when set vertical. The simplest situation is obtained for insoluble surfactants where  $\Gamma_1 \neq 0$  and  $c_1 = 0$ . Then, using eqs. (2), (3) and (5) together with (18)

the thickness is given by

$$e(z) = e^* \exp \left[ -\frac{\rho g e^* z}{2(\sigma_0 - \sigma^*)} \right]. \quad (19)$$

This thickness profile, shown on fig. 3(a), is the equivalent of the density profile of an isothermal atmosphere. The only difference is that, in the atmosphere the gas carries its own weight only, whereas here, the soap molecules carry the interstitial fluid as well. As a result, at room temperature, the vertical variation of the density is much larger, and a 20 cm high soap film simulates an atmosphere a few kilometers thick.

For small concentrations of a soluble soap, Rusanov and Krotov [5] using (9) find

$$\frac{de}{dz} = -\frac{\rho g e e^* (e + 2k)^2}{4k(\sigma_0 - \sigma^*)(e^* + 2k)} \quad (20)$$

and the thickness is given by the implicit relation

$$z = \frac{(\sigma_0 - \sigma^*)(e^* + 2k)}{\rho g k e^*} \times \left( \frac{e}{e + 2k} - \frac{e^*}{e^* + 2k} - \ln \frac{e(e^* + 2k)}{e^*(e + 2k)} \right). \quad (21)$$

Fig. 3 shows two thickness profiles calculated from (19) and (21) respectively. These equations give possible instantaneous profiles of films; they have been found taking  $e^*$  and  $\sigma^*$  to be constant, an assumption which is equivalent to considering that the total quantity of fluid of the film is constant. In fact drainage occurs and some fluid is transferred to the frame so that  $e^*$  and  $\sigma^*$  vary slowly with time. Experimentally most usual soaps are made of several components, the equation of state is more complicated and the profiles of fig. 3 are

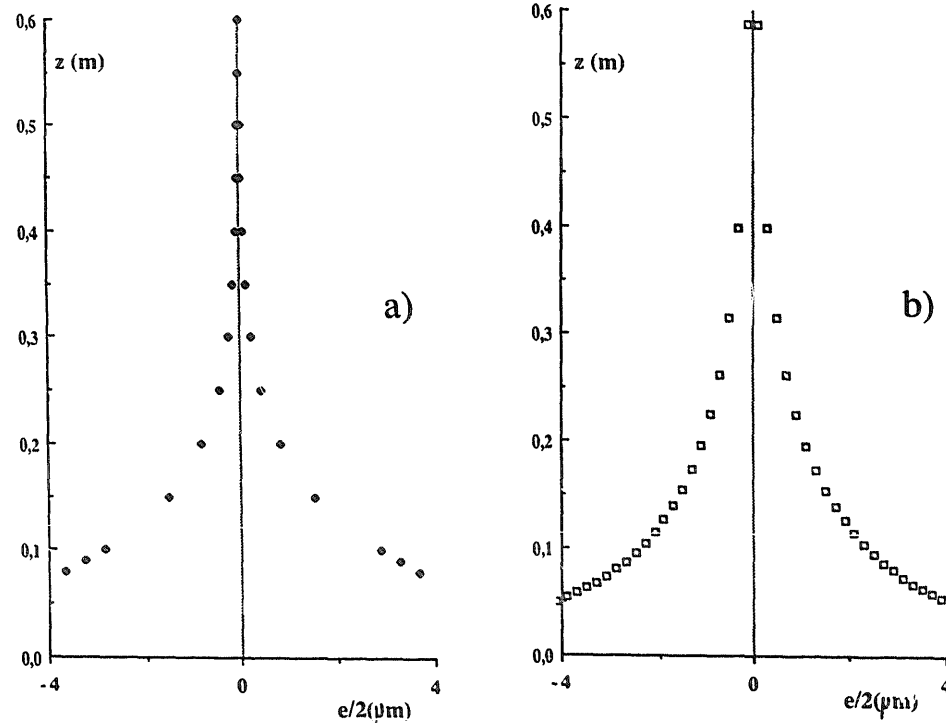


Fig. 3. Thickness profiles of a vertical film as a function of height  $z$ : (a) deduced from eq. (19) (with  $k/e^* = 0.4$ ), (b) deduced from eq. (21).

only two among a large variety of observed thickness profiles.

Finally if, instead of being vertical, the film is set inclined at an angle  $\alpha$  with the vertical, the component of the weight normal to the surface gives it a slight curvature. The equilibrium gives the resulting local radius of curvature  $R_0$ :

$$R_0 = \frac{dz}{d\alpha} = \frac{2\sigma(z)}{\rho e(z)g \sin(\alpha)}. \quad (22)$$

For a film 2  $\mu\text{m}$  thick at  $\alpha = 60^\circ$ ,  $R_0 \approx 5$  m. In the following we will neglect this curvature and consider the film as plane. The equilibrium in the plane of the films is then the same as that of a vertical film but, with a reduced gravity  $g' = g \cos \alpha$ . Eq. (17) becomes

$$2 \frac{d\sigma}{dz} = \rho g' e(z). \quad (23)$$

#### 4. Soap films set into motion by an air flow

The previous discussion of the physical properties of soap films was a necessary preliminary to the description and understanding of fluid dynamics experiments performed in soap films. The interaction of the film with the surrounding air is a dominant feature of these experiments and we will treat separately the experiments where the flow is dominated by the inertia of air or by that of the film. We will first describe two experiments where the film is set into motion by an air flow.

##### 4.1. Interaction of a film with a two-dimensional air flow

A soap film is easily dragged into motion by an air flow parallel to its surface (Couder et al. [6], Rabaud and Couder [7] and Chomaz et al. [11]). The film then provides an excellent visualization of the flow. We had investigated a shear in a

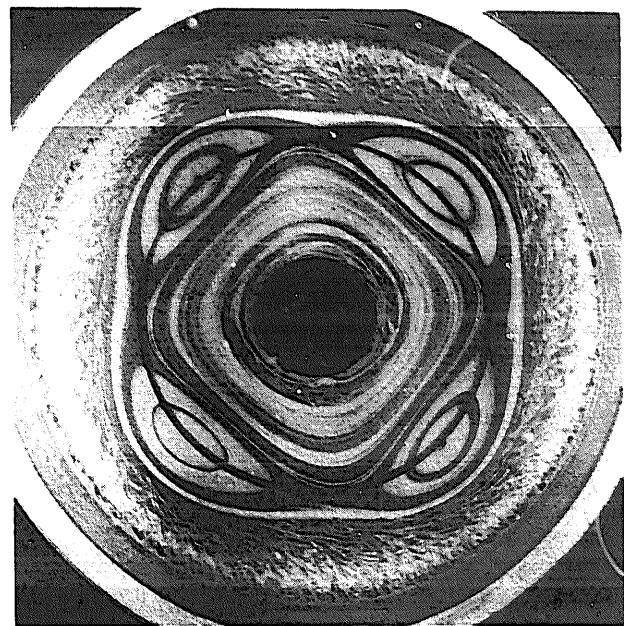


Fig. 4. The interference fringes of a film in a circular shear flow, showing four co-rotating vortices.

cylinder of very small height in which the air was set into two concentric circular motion. A steady pattern of regular vortices was created in the cell. For symmetry reasons the air flow in the central plane of the cell was two-dimensional and the introduction of a soap film in this plane did not disturb it. As the film has a small kinetic viscosity, it was easily set into motion. Whenever the air flow was steady, the film drained slowly and reached thickness profiles which were related to the pressure distribution. Fig. 4 shows the observed interference fringes; in the central region, as well as around each vortex core, concentric fringes were observed.

In a two-dimensional system, rotating at angular velocity  $\omega$ , the centrifugal forces are usually expressed as the gradient of a scalar quantity  $\frac{1}{2}\omega^2 r^2$  where  $r$  is the distance to this axis of rotation. In an enclosed classical fluid this term is balanced by a radial pressure gradient and the situation is analogous to the equilibrium in the gravity field. Submitted to the centrifugal forces, a soap film in rigid rotation is in a state similar to the quasi equilibrium described in section 3. Ob-

served over a long time the fringes move slowly outwards. This is only due to the very slow Poiseuille flow of the interstitial fluid. If it is neglected, each element of a film in solid rotation is in a Gibbs quasi equilibrium which can be described in polar coordinates using the spreading pressure  $f$ :

$$2\left(\frac{df}{dr} + \frac{f}{r}\right) = \rho e(r)\omega^2 r. \quad (24)$$

In the shear flow experiment, the film thickness results from the superposition of the centrifugal forces due to the rotations around the center and around the vortices.

In unsteady regimes the film still shows the structure, but the visualization is of a different type. If the time scale of the motion is too short for the equilibrium to settle, the regions of different thickness are advected by the flow as if they were an unevenly spread passive scalar.

#### 4.2. Interaction of a film with a three-dimensional air flow

Observation of a soap bubble shows that it is very sensitive to the drafts of the surrounding air. To investigate the interaction of the three-dimensional motion of air with the film we set a simple experiment where a thin air jet impinges on a plane film. It is rather surprising that we did not find a description of this experiment in the literature with the sole exception of an allusion in an article by Kitchener and Cooper [19] who quote it as an imaginary experiment for pedagogical presentation of the film elasticity.

The soap film is stretched on a horizontal circular rim, at a distance  $h$  ( $h \approx 1$  cm) above a compartment in the center of which one single hole 0.5 mm in diameter is pierced. By this hole air escapes in a thin jet perpendicular to the film's surface. The soap film shows a slight bulge at the point where the air jet impinges on its surface. The

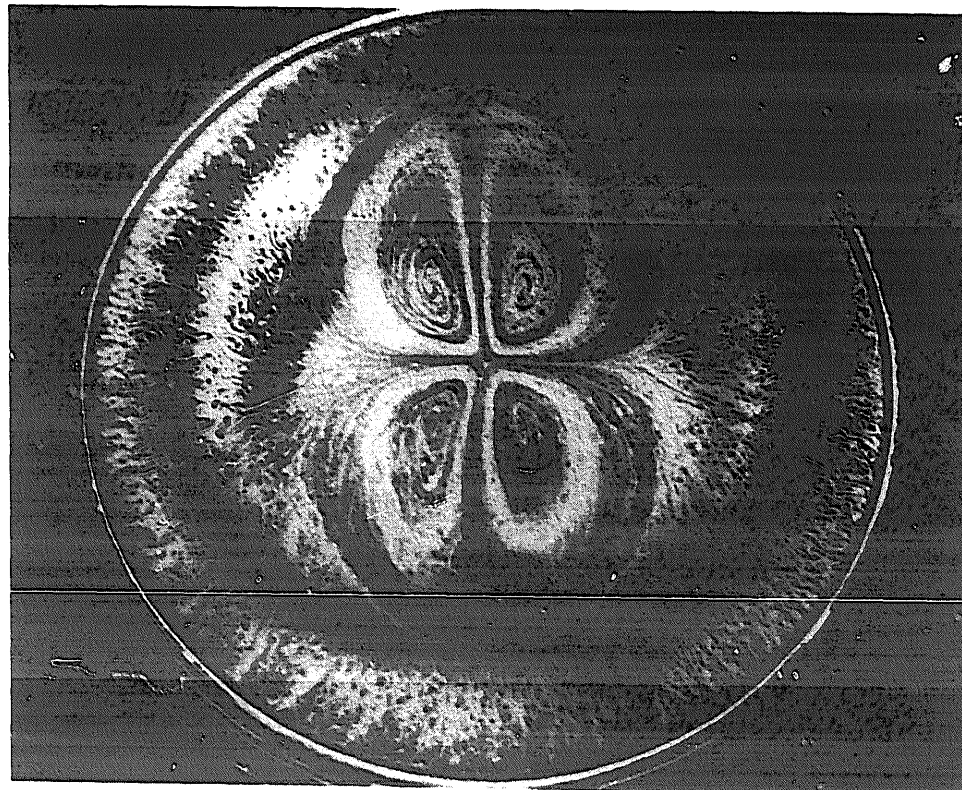


Fig. 5. The circulations observed in a horizontal film, when an air jet impinges perpendicularly to its surface. This picture shows the two outwards and the two inwards flows.

observation of the film in monochromatic light shows fast motions in its surface. The axisymmetry of the system is broken, and the axis of the jet become a saddle point separating four regular steady circulations (fig. 5). They result from two effects; the deflected air flow drives the film in a radial outward motion, but the local increase of the surface tension due to the stretching and thinning of the film, tends to create a radial inward motion of the film. These two opposite effects break the axisymmetry of the system. The air motion creates in the film plane two strong thin opposite radial jets while the surface tension gradient generates large recirculations of fluid towards the center.

If the jet is not initially perpendicular to the surface the axisymmetry does not exist initially and only two circulations are observed.

This experiment clearly demonstrates the stabilizing influence of the film's elasticity that we described in section 2.4. From the two preceding experiments we can also deduce the boundary conditions that are imposed (in a steady regime) to the velocity  $u_{\text{air}}$  of an air flow at the surface of the film:

$$\begin{aligned} (u_{\text{air}})_\perp &= 0, \\ (u_{\text{air}})_\parallel &\neq 0, \\ (\text{div } u_{\text{air}})_\parallel &= 0, \end{aligned} \quad (25)$$

as the film surface is incompressible in stationary regimes. These conditions show that the air flow is two-dimensional near the film.

## 5. Flows in a horizontal film

In this paragraph we will investigate the situation where a flow is generated directly in the film. The surrounding air, initially motionless, is only set into motion by the flow in the film. Experiments of this type had been undertaken by us to investigate turbulent flows in a nearly two-dimensional medium. We limited ourselves to decaying turbulence in which energy is provided to the system at an initial time. In our first series of experiments [8] we showed that grid turbulence could be generated by towing in the film a comb formed of regularly spaced cylinders. They created parallel interacting wakes in which the vortices grew in time by pairing processes (fig. 6). The growth of the vortices size was linear in time, a behavior predicted for two-dimensional decaying turbulence [22].

We also investigated the two-dimensional evolution of a turbulent wake. In this case to make the system as two-dimensional as possible we towed a disk of aluminum paper ( $8 \mu\text{m}$  thick) suspended in

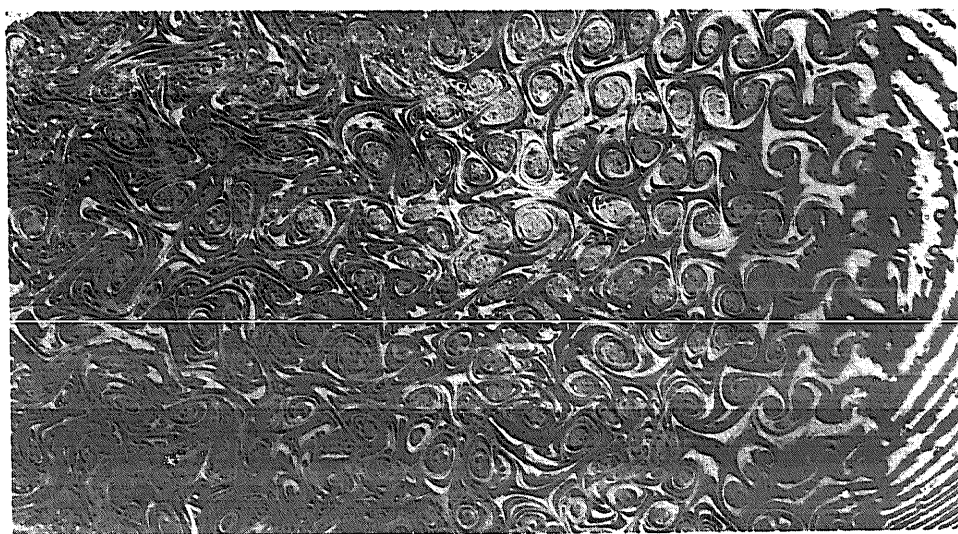


Fig. 6. Grid turbulence in a soap film (the cylinders are moving from left to right).

the film [12]. It was held by two thin needles which had a negligible wake in the air. Depending upon its velocity, we observed in the films the various types of wakes that a long cylinder produces in a classical fluid. A difference appears at large velocity because in classical fluid the Von Karman wake becomes three-dimensional and turbulent. In the soap film it retains its two dimensionality. We showed [12] that two modes were observed. In the first one (fig. 7(a)) the destabilization occurs through pairing and merging of likewise vortices [20]. The growth in size of the vortices, which are the energy carrying structure, is observed directly. This phenomenon is the elementary process of the inverse energy cascade and characterizes two-dimensional turbulence. At larger velocities (fig. 7(b)) we observe the formation of singular structures formed of two vortices of opposite sign. These couples are very fast and move into the quiescent zones of the fluid, thus diffusing turbulence. Both processes, the pairing and the formation of couples, have been observed in numerical simulations [21, 12] and are intrinsic features of two-dimensional flows.

In these experiments, however deviations were observed from a strict two-dimensional behaviour. In both the grid and the wake turbulence a general damping of the motion of the structures of all scales was observed at large time and ascribed to the effect of air friction. This friction also affects the threshold at which a Von Karman wake is formed in the film. In normal fluids it occurs at a threshold value of the Reynolds number based on the velocity  $v$  and the diameter  $D$ . For various cylinders the product  $vD$  is constant at threshold. In soap film it increases with  $D$ . Furthermore it is also a function of the film thickness. This manifests the fact that we must consider two frictions: the viscous friction in the film and the damping due to the surrounding air.

In section 5.1 we discuss the equations of motion of soap films and show under which restrictions they can be considered as those of incompressible two dimensional flows. In section 5.2 we give an estimate of the effect of the air friction.

### 5.1. Equation of motion

For the reasons discussed in section 3, the flow of inner regions of the film relative to the surfaces is very slow. We will neglect it completely here and only consider motions in which an element of the film moves as a whole.

We will particularly discuss in which conditions the motion includes local stretching, in other terms whether or not the fluid behaves as an incompressible two-dimensional fluid. We will first limit ourselves to a model situation where the film at rest is horizontal, has constant thickness  $e^*$  and surface tension  $\sigma^*$ , and where the concentration in soap is small.

The equations of motion of an element of a horizontal film of thickness  $e$  are the Navier-Stokes equation, the equation of conservation of the fluid and the equation of conservation of soap. (The later gives the film its elasticity.)

In the Navier-Stokes equation the usual pressure term is replaced by surface tension and can be written

$$2\nabla\sigma = \frac{2d\sigma}{de} \nabla e = -\frac{E(e)}{e} \nabla e. \quad (26)$$

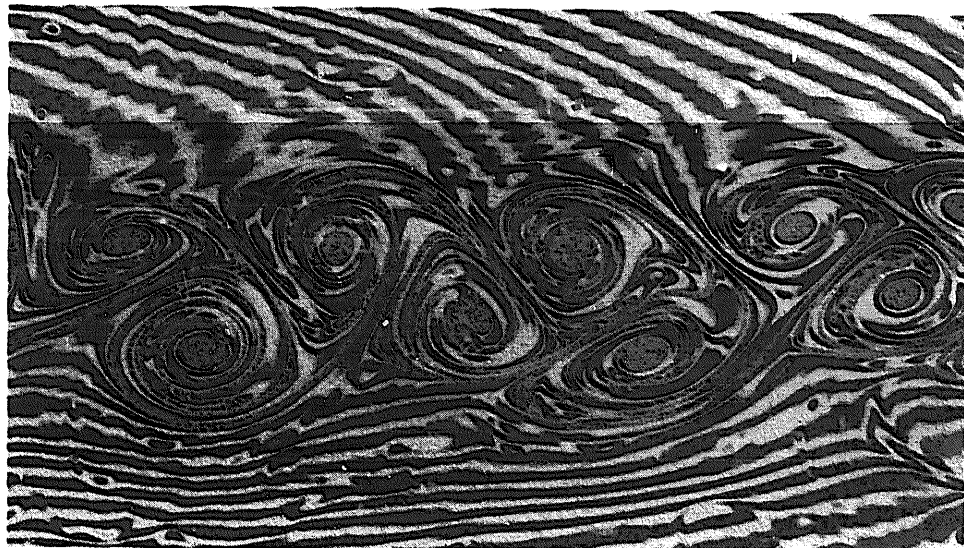
We will write as  $F_f$  the sum of all the damping terms due to the film's viscosity and to the air friction. These will be discussed separately in the next paragraph. We then have

$$\left. \begin{aligned} \frac{Du}{Dt} &= -\frac{E(e)}{\rho e^2} \nabla e + \frac{F_f}{\rho e}, \\ \frac{De}{Dt} &= -e \operatorname{div} u, \end{aligned} \right\} \quad (27)$$

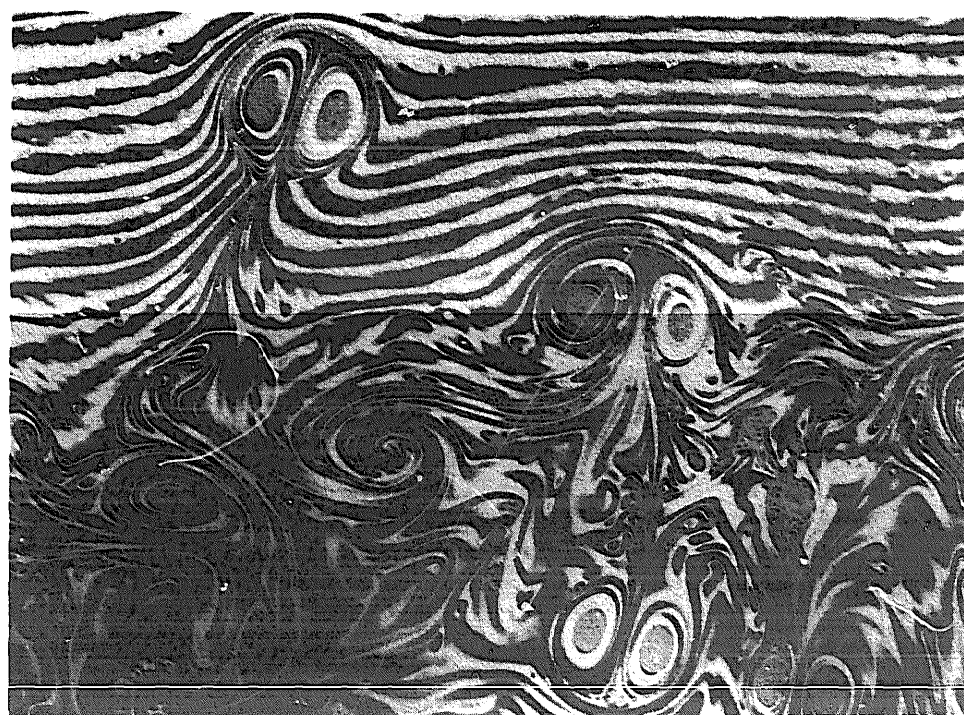
where the operator symbolized by  $D/Dt$  is the substantive derivative ( $D/DT = \partial/\partial t + u \cdot \nabla$ )

On short times scales the elasticity  $E(e)$  to be considered is the Marangoni elasticity given by eqs. (8) and (9). It is related to the film thickness by

$$E_M(e) = E_M(e^*) \frac{e}{e^*}, \quad (28)$$



(a)



(b)

Fig. 7. The two modes of destabilization of a Von Karman wake: (a) by pairing of vortices of the same sign, (b) by formation of couples of vortices of opposite signs.

where  $e^*$  is the thickness of the film at rest. We will then say in short that the film has a Marangoni dynamics.

On longer times scales the film has a Gibbs dynamics and its elasticity is given by eq. (10) so that

$$E_G(e) = E_G(e^*) \frac{e}{e^*} \left( \frac{e^* + 2k}{e + 2k} \right)^2. \quad (29)$$

Eqs. (27) are those of the motion of a two-dimensional compressible fluid of surface density  $\rho e$ . The propagation of elastic waves is the equivalent of propagation of sound waves in a normal fluid: their velocity  $v_{LF}$  is given by (16). In the following, we introduce a dimensionless number  $M$  which is analogous to the Mach number:

$$M = \frac{u}{v_{LF}} = u \sqrt{\frac{\rho e^*}{2E(e^*)}}. \quad (30)$$

We can scale  $u$  by  $U$ ,  $x$  by  $L$ ,  $t$  by  $L/U$  and write  $e = e^*(1 + M^2 e')$ . If we assume a Marangoni dynamics, eqs. (27), when written in an adimensional form, become

$$\begin{aligned} \frac{Du}{Dt} &= - \frac{\nabla e'}{1 + M^2 e'} + F_f \frac{L}{U^2 e^* \rho (1 + M^2 e')} , \\ \frac{De'}{Dt} &= - \frac{1 + M^2 e'}{M^2} \operatorname{div} u. \end{aligned} \quad \left. \right\} \quad (31)$$

If the dynamics is of a Gibbs type,

$$\begin{aligned} \frac{Du}{Dt} &= - \frac{\left(1 + \frac{2k}{e^*}\right)^2}{(1 + M^2 e') \left(1 + M^2 e' + \frac{2k}{e^*}\right)} \nabla e' \\ &\quad + F_f \frac{L}{U^2 e^* \rho (1 + M^2 e')} , \\ \frac{De'}{Dt} &= - \frac{1 + M^2 e'}{M^2} \operatorname{div} u \end{aligned} \quad \left. \right\} \quad (32)$$

The elastic wave velocity (section 2.5) is of the order of a few meters per second. In experiments

reaching large velocities the dynamics of the film would be that of a compressible two-dimensional fluid and would, on short time scales, be described by eqs. (31). In the experiments that we describe in the present article the fluid velocity is smaller than the wave velocity.  $M^2$  is thus small and, at first order in  $M^2$ , eqs. (31) or (32) reduce to

$$\begin{aligned} \frac{Du}{Dt} &= - \nabla e' + F_f \frac{L}{U^2 e^* \rho}, \\ \operatorname{div} u &= 0. \end{aligned} \quad \left. \right\} \quad (33)$$

## 5.2. Damping terms

### 5.2.1. Film viscosity

The first dissipative term in eqs. (27) is the viscous friction in the film plane

$$F_{f1} = \frac{\mu_F^S}{\rho e} \nabla^2 u, \quad (34)$$

where  $\mu_F^S$  is the surface viscosity of the film. The interstitial fluid has the viscosity of pure water  $\mu_W$  but the two superficial layers [4] have a specific surface viscosity  $\mu_S^S$  which depends on the nature of the soap and on its concentration. The resulting surface viscosity is

$$\mu_F^S = e \mu_W + 2 \mu_S^S. \quad (35)$$

In the films we used,  $\mu_S^S$  is of the order of  $10^{-8}$  kg/s (valid quantitative data on this parameter are very difficult to find in the literature).

The ratio of the inertial forces to these viscous forces is a Reynolds number:

$$Re = \frac{\rho e U L}{\mu_W e + 2 \mu_S^S}, \quad (36)$$

which depends on the film thickness.

### 5.2.2. Damping by air

If the film is set into motion in a motionless air, two boundary layers of thickness  $\delta$  grow on each side of the film. The friction of a fluid on a

translating plate impulsively started is treated in Landau and Lifshitz [23]. It is expressed as a function of the derivatives of the velocities at earlier times. We will limit ourselves here to an estimate of this effect.

We write that the velocity gradient is extended over the thickness  $\delta$  of the boundary layer:

$$\delta = \sqrt{\nu_a t} \approx \sqrt{\nu_a \frac{L}{U}},$$

where  $\nu_a$  is the kinematic viscosity of air,  $\rho_a$  its density. The order of magnitude of the resulting friction on the film is

$$F_{f2} \approx \frac{2\rho_a \sqrt{\nu_a} u^{3/2}}{\sqrt{L}}. \quad (37)$$

The ratio of the inertial forces to this dissipative term is

$$C = \frac{\rho e \sqrt{U}}{2\rho_a \sqrt{\nu_a L}}. \quad (38)$$

We can compare the two dissipations by writing their ratio:

$$\frac{F_{f2}}{F_{f1}} = \frac{2\rho_a \sqrt{\nu_a U L^3}}{\mu_w e + 2\mu_s^2}. \quad (39)$$

This gives the interpretation of the anomalous thresholds observed for the formation of the Von Karman wake. In the range of diameters that we use,  $L = 0.1$  cm to  $L = 1$  cm, there is a crossover between the two dissipative processes. It is only for small diameters in thick films, that the Reynolds number retains its critical role. For large disks the viscous dissipation in air becomes dominant, so that the wake only appears when a critical value of  $C$  is reached.

It is possible to reduce this effect by towing a long cylinder in a film immersed in a gas of a kinematic viscosity value close to that of the film. (This is almost realized using sulfur hexafluoride, a gas of large density.) A similar wake is

simultaneously created in the film and the gas so that the shear in the gas near the film is reduced. Even though the wake is three-dimensional in the gas it is forced to remain two-dimensional in the vicinity of the film.

## 6. Surface tension driven buoyancy

A vertically stretched soap film is in a particular state of quasi equilibrium (described in section 3) where a surface tension gradient opposes the influence of gravity. The effect of this gradient is equivalent to that of a two-dimensional hydrostatic pressure and we can obtain the two-dimensional equivalent of some classical three-dimensional buoyancy experiments.

### 6.1. A two-dimensional balloon

We first repeat a popular demonstrative experiment showing the effect of surface tension (Plateau [1] or Boys [3]). We knot both ends of a fine thread (e.g. a thin hair of diameter  $30 \mu\text{m}$ ) to form a closed loop which we place in the soap film. Breaking the enclosed part of the film, the surface tension of the outer film gives a circular shape to the loop and we obtain a circular hole bordered by the thread.

Placed in a vertical frame this hole will be submitted to two forces; its weight  $mg$  (where  $m$  is the mass of the thread plus the mass of the attached meniscus) and a buoyancy force equal to the weight of the excluded surface of fluid. The resulting force is

$$F = mg - \rho g \iint_{\text{loop}} e(z) dy dz. \quad (40)$$

If the film is set inclined at an angle  $\alpha$  with the vertical, the in-plane forces will have the same expression, replacing  $g$  in (40) by  $g' = g \cos \alpha$ .

When the loop is placed at the bottom of the frame where the film is thickest, there is a buoyant force and the loop moves upwards. During this



Fig. 8. A photograph showing the rising motion of a loop of diameter 1.9 cm in a vertical film and the aspect of its wake.

motion the surrounding film becomes thinner and the loop loses its buoyancy until it becomes motionless at a level of equilibrium where  $F = 0$ . This motion is exactly similar to that of a balloon rising in the stratified atmosphere where the density decreases with height. We have here an experimental demonstration of the similarity of the equilibrium of a vertical film with the equilibrium of the atmosphere discussed above (see eqs. (19) and (21)).

Fig. 8 shows the motion of a hole of diameter  $d = 1.9$  cm rising in a film inclined with  $\alpha = 60^\circ$ . The velocity of rise is 9 cm/s, and the Reynolds number is  $Re \approx 200$ . For this value the wake of an infinite cylinder moving in a bulk fluid is characterized by direct alternate shedding of vortices behind the cylinder forming a Von Karman street.

During its ascent the hole has an oscillatory motion, where it simultaneously rotates and sideslips alternatively on one side and the other, in reaction to the alternate emission of vortices. The wake behind the loop tends to engulf regions of larger thickness in thinner regions; gravity will then tend to bring back each region at its equilibrium level. This leads to a rapid collapse of the vortices which form motionless regions of disordered medium. This effect is classically observed in experiments on bulk stratified fluids, where the collapsed zones are often called *billows*.

## 6.2. The buoyant motion of two-dimensional "bubbles"

The film is formed of a solution of concentration  $c_0$  which remains constant and characterizes the fluid. It is possible to create, at will, zones of a different two-dimensional density by touching the film with a needle covered with pure soap. A local larger soap concentration  $c'_0$  is thus created. The surrounding film stretches rapidly this region where the surface tension has been lowered. This stretching will continue until the surface concentration  $\Gamma_1$  has decreased restoring a value of surface tension in equilibrium with the surrounding film. This process creates a thinner zone with a constant thickness  $e_2$ . If the frame is horizontal the zone is circular. The creation of these thin zones is difficult to control: the quantity of soap deposited by the needle is variable and the efficiency of the process seems to depend upon the difference in pH between the film and the pure soap. Whenever too much soap is deposited the stretching can be so large that no equilibrium is reached until the whole film on the frame is replaced by black film. Depending on the type of soap that is used this thickness corresponds either to one of the black films ( $e_2 \approx 4.5$  or 30 nm) or to the silvery white of the first light fringe ( $e_2 \approx 100$  nm). The limit between the thin zone and the film is sharply defined. A tentative description of the probable aspect of the rim is given on the sketch of fig. 9. When the zone is no longer spreading the

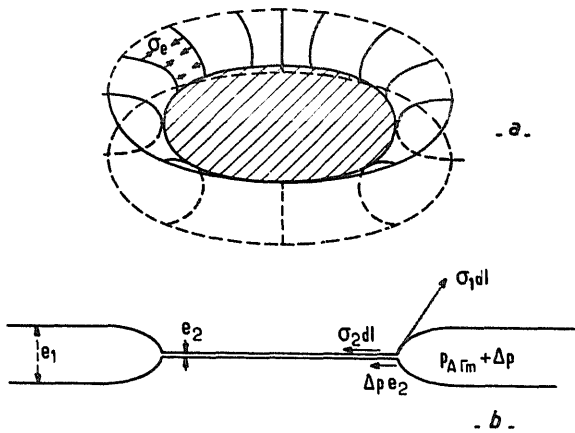


Fig. 9. Sketches of the shape of the rim of thicker fluid surrounding a thin zone.

radial equilibrium of the rim can be written

$$2\sigma_1 \cos \theta = 2\sigma_2 - \Delta p e_2, \quad (41)$$

where  $\sigma_1$  and  $\sigma_2$  are the surface tensions of the surrounding film and of the thin zone respectively,  $\theta$  the angle of contact and  $\Delta p$  the Laplace pressure jump on the rim due to its curvatures. The rim's radius of curvature in the film plane is large, but in the perpendicular direction we can probably assume that it is of the order of the film thickness so that  $\Delta p \approx \sigma_1/e_1$  and the pressure term, though small, is probably not negligible. This, together with the fact that  $\theta$  is probably large, shows that at equilibrium  $\sigma_2 < \sigma_1$  and the surface concentration of soap remains larger in the zone than outside.

These zones, once created, are stable and behave as if they were formed of a different, immiscible fluid. Restoring a thickness comparable to that of the surrounding film would require that interstitial liquid flows back between the superficial layers; a Poiseuille flow of that kind would be extremely slow and, in the case where the zone is black, the interaction between the two surfaces opposes any thickening.

The circular shape of the zones at rest shows that there exist a line tension  $\lambda$  around these zones. This line tension can result simply from the normal surface tension acting on the side of the

rim out of the film's plane (fig. 9a). In this case it would be

$$\lambda = \sigma_1(e_2 - e_1). \quad (42)$$

There can also be corrections due to the contact line itself. We did not find quantitative data about  $\lambda$ .

Created near the bottom of the frame and surrounded by thicker fluid these zones are submitted to a buoyant force:

$$F = \rho g \left[ e_2 S - \iint_S e(z) dy dz \right],$$

and rise up in the frame until they reach the level where  $e(z) = e_2$ . The velocity of their motion as well as their shape during the ascent is the two-dimensional equivalent of the motion and the shape of rising bubbles in a classical fluid.

A large number of articles have been devoted to the shape of bubbles and drop. Reviews of this subject can be found in Harper [24], Wegener and Parlange [25], Clift et al. [26]. An article by Bhaga and Weber [27] also gives an extensive study of the subject.

The case of plane bubbles, which is particularly relevant for comparison to our experiments, was studied experimentally in normal fluids enclosed in a Hele Shaw cell. Results in this type of geometry were obtained by Walters and Davidson [28], Collins [29], Grace and Harrison [30], Crabtree and Brigwater [31], Hills [32] and Maxworthy [33].

In normal fluids the shape of rising bubbles and the nature of their wakes are usually described as a function of a set of several parameters representing the relative importance of buoyancy, inertia, viscosity and surface tension. Various sets of parameters are in use. One of the most usual is formed of the Reynolds number of the motion, the Eötvös number which is the ratio of buoyancy over capillary forces and the Morton number which characterizes the fluid. They are defined as

follow [26]:

$$\text{Re} = \frac{\rho d_e U}{\mu}, \quad \text{Eo} = \frac{g \Delta \rho d_e^2}{\sigma}, \quad \text{Mo} = \frac{g \mu^4 \Delta \rho}{\rho^2 \sigma^3}, \quad (43)$$

where  $d_e$  is the diameter of the sphere of equivalent volume.

In order to keep to those number the same significance in our two-dimensional case, they must be modified.  $\Delta \rho$ , the difference in density between the two fluids, is here  $\rho(e_2 - e_1)$ . The equivalent of the interfacial tension  $\sigma$  is the line tension  $\lambda$ . The viscosity  $\mu$  must be replaced by the film surface viscosity  $\mu_F^S$  given by relation (35). Instead of being the diameter of the volume equivalent sphere,  $d_e$  is the diameter of the surface equivalent circle. The gravity acceleration,  $g' = g \cos \alpha$ , takes into account the possibility of working in inclined films. The numbers become

$$\begin{aligned} \text{Re} &= \frac{\rho e_2 d_e U}{2\mu_S^S + \mu_W e_1}, \\ \text{Eo} &= \frac{g' \rho (e_2 - e_1) d_e^2}{\lambda}, \\ \text{Mo} &= \frac{g' \rho (2\mu_S^S + \mu_W e_2)(e_2 - e_1)}{\rho^2 e_2^2 \lambda^2}. \end{aligned} \quad (44)$$

In the case where  $\lambda$  is given by relation (42), the Eötvös number simplifies and becomes independent of the film thickness:

$$\text{Eo} = \frac{\rho g' d_e^2}{\sigma_2}. \quad (45)$$

Clift et al. [26] give in classical fluids a plot of the Reynolds number and shape of bubbles as a function of their Eötvös number. This dependence is parametrized by the Morton number of the fluid. In soap films the situation is more complicated because the liquid is very strongly density and viscosity stratified. For a given bubble, both the Reynolds number and the Morton number change during the ascent. The Eötvös number is

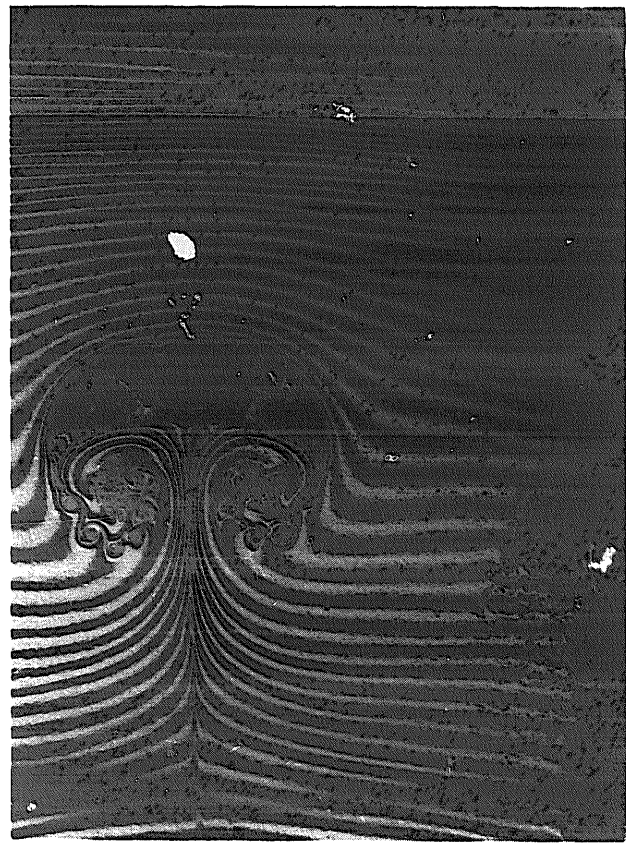


Fig. 10. Shape of a rising black zone shortly after its creation. The indentation at the top of the spherical cap corresponds to the initial stage of development of a Rayleigh-Taylor instability (which will at later times split the zone). Secondary vortices created by the shear roll up to form the main trailing vortices. The maximum width of the black zone,  $d = 3$  cm, gives the scale. (The marginal regeneration is also visible on the vertical border of the frame.)

only constant if it is given by eq. (45). As a result there is a constant evolution of the bubble shape. Though we did not investigate this point systematically we observed that roughly the various regimes correspond to those given by the diagram of Clift et al. [26]. Zones of small area, rising in a thin film, are circular or elliptical while larger zones rising in thicker film have a spherical cap shape.

The initial motion for large zones corresponds to the formation of a circular cap with two attached trailing vortices. The distortion is very rapid and corresponds to the description of Walters and Davidson [28], figs. 10 and 11 show this shape. The top part of the bubble becomes circular and

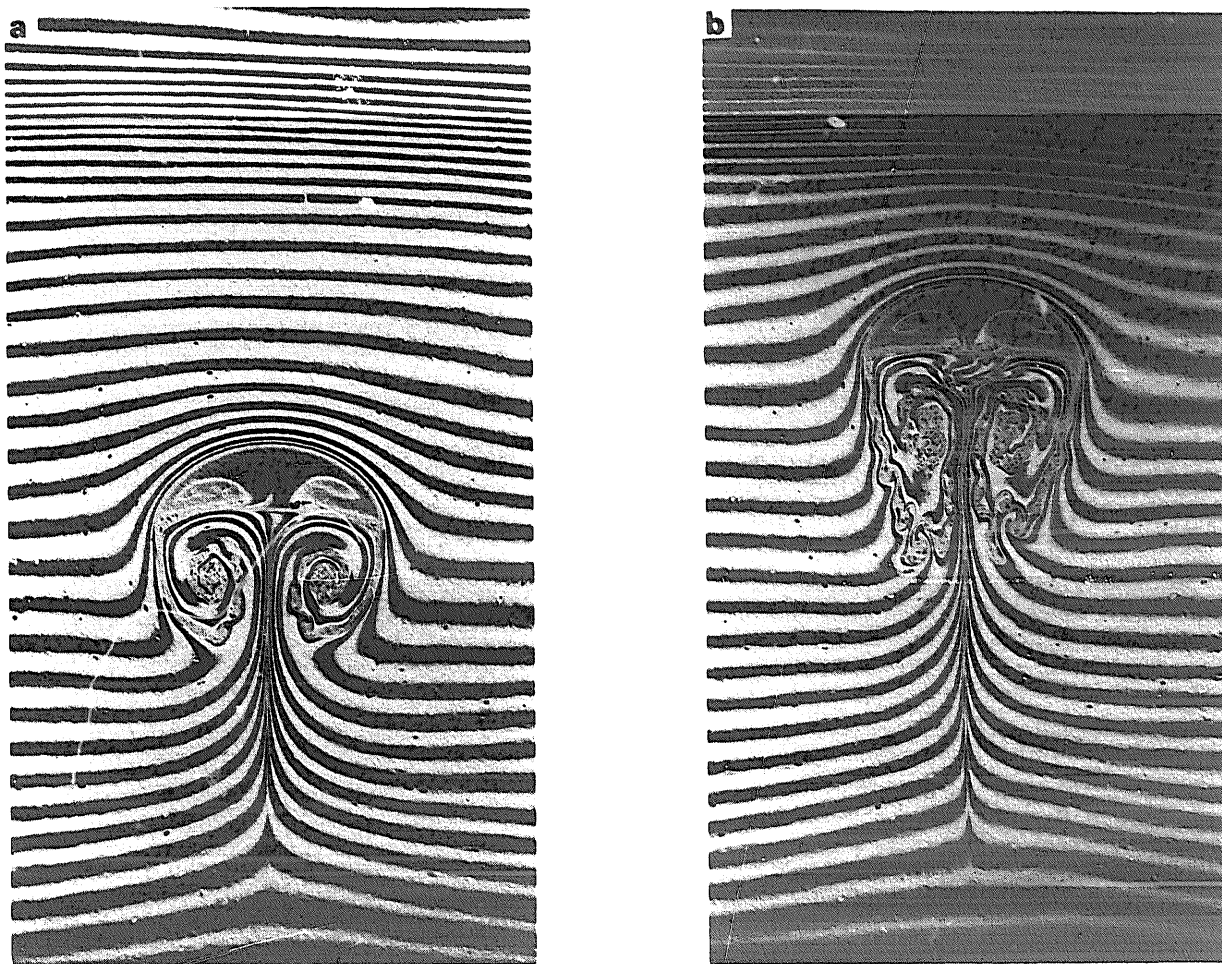


Fig. 11. Three stages at times  $t = 0.6, 0.9$  and  $1.2$  s of the rise of a thin zone, showing the detachment of the trailing vortices.  
(Continued on next page.)

the shear near the edge gives rise to two lines of vortices which roll up into two large trailing vortices.

Figs. 11 (a, b and c) show the later evolution of the wake. The two trailing vortices are formed with thick film collected at the early stage of the rising motion; they become unstable as the bubble moves up to thinner regions, they detach and fall down.

Davies and Taylor [34] showed that the spherical shape of the upper surface of three-dimensional bubbles corresponds to an equilibrium of the dynamic pressure at the interface. They found a relation between the radius of curvature of the sphere and the limit velocity of ascent. In two

dimensions the corresponding relation derived by Collins [29] is

$$U_T = 0.5 \sqrt{gR \frac{\Delta\rho}{\rho}} ; \quad (46)$$

adapted for soap films it is

$$U_T = 0.5 \sqrt{g'R \frac{(e_2 - e_1)}{e_2}} . \quad (47)$$

We measured local velocities and curvatures of ascending spherical caps and find that they do satisfy relation (47) to the uncertainty of the measures.

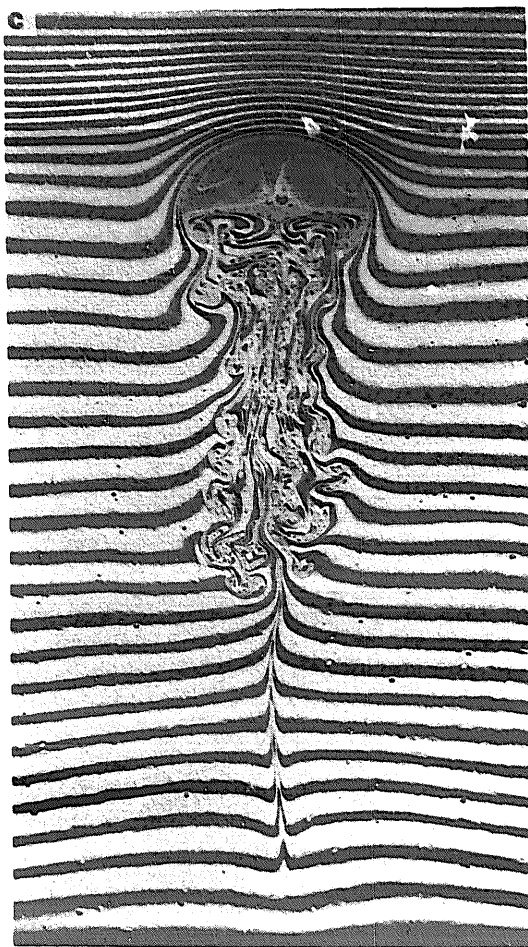


Fig. 11. Continued.

Finally a specific effect is observed when the bubbles reach the upper regions of the film. As their buoyancy decreases, the bubbles become unstable and repeatedly break into two. Fig. 12 shows the four bubbles resulting from two successive splitting.

This effect is not well understood. Classical bubbles usually break due to the Rayleigh–Taylor instability. Clift et al. [26] give an upper limit for the size of stable bubbles:

$$d_c = 2\pi \sqrt{\frac{\sigma}{g\Delta\rho}} . \quad (48)$$

In soap film  $\sigma$  must be replaced by the line tension which is not well known. If it satisfies relation (42) then  $d_c$  does not depend on the film's

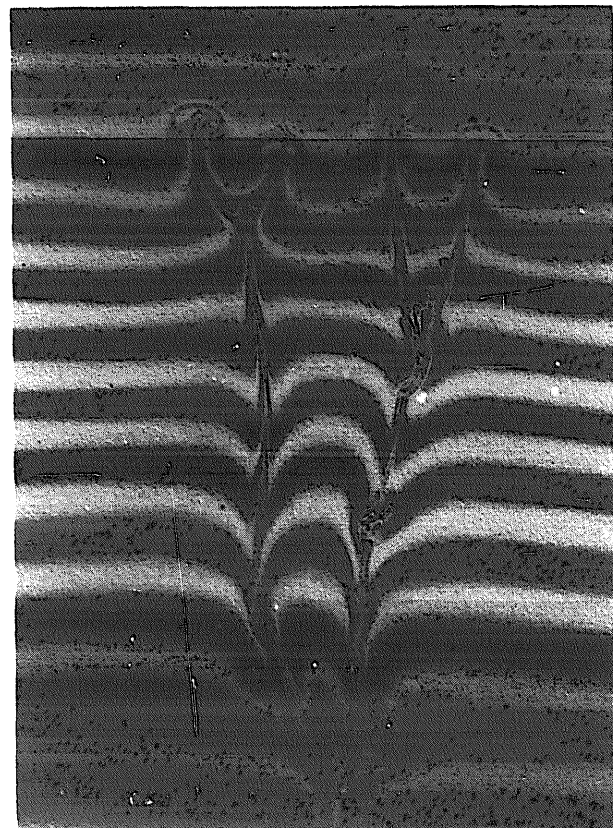


Fig. 12. The four zones resulting from two successive splittings. The falling back of thick zones dragged by the wake creates oscillations of the stratified fluid.

thickness which seems unrealistic. Another possibility is that, as the buoyancy decreases, so does the bubble velocity, so that the Davies and Taylor equilibrium is destroyed and the bubble breaks.

### 6.3. Internal waves

In the preceding paragraphs we have investigated the buoyancy of artificially introduced extraneous immiscible objects. In the present part we will examine the possibility that a stable stratified state of a vertical film can propagate internal waves.

Let us consider a vertical film in a Gibbs equilibrium (of the type described in section 3) and a motion which displaces upwards an element of the film. The surface tension in this element becomes smaller than in the surrounding film and it is

submitted to an elastic stretching. This stretching can be of the Gibbs type, in this case the film element always remains in equilibrium with its surroundings and there will be no restoring force. On the other hand if the stretching is of the Marangoni type, the element, when the equilibrium of surface tension is reached, is still thicker and heavier than the surrounding film. It will be submitted to a restoring force and will possibly oscillate with a Brunt–Väisälä frequency.

In a soap film this frequency will be

$$N = - \sqrt{\frac{g'}{e(z)} \frac{de}{dz}}. \quad (49)$$

In principle the time scale over which the elasticity is considered to be of a Gibbs type are shorter ( $\sim 10^{-2}$  s) than the expected period ( $\sim 1$  s) of the internal oscillation, so that no wave should be observed. As discussed above, other results hint towards a much longer time for a Gibbs equilibrium to establish in the case of complex solutions.

To settle which is the actual situation, we repeated in a soap film the lee wave experiments first performed by Long [35] of which a complete theoretical treatment was done by Miles and Huppert [36]. We tow in the lower part of an

inclined film a large disk of aluminum paper of radius  $R_1$  ( $R_1 = 3$  cm) at a velocity  $U$ . The frame on which the film is stretched has a width  $H$  ( $H \gg R_1$ ). Varying the velocity of the disk we change the Froude number of the flow

$$Fr = \frac{U}{NR_1}. \quad (50)$$

Theory predicts [36] that the waves increase in amplitude when the Froude number decreases. A critical value  $Fr_c$  is defined as the value for which the wave reaches such a large amplitude that a density inversion appears at a point of the flow. In the geometry that we consider, Miles and Huppert [36] found  $Fr_c = 0.787$ .

The observed patterns in soap films are in good agreement with the prediction for both the Brunt–Väisälä frequency and the critical Froude number. Fig. 13 shows the interference fringes behind a disk moving with  $Fr$  slightly below  $Fr_c$ . Their aspect is in very good agreement with the streamlines calculated by Miles and Huppert [36], and an inversion of density is observed.

This observation confirms that over periods of time of the order of a second or more, a Marangoni dynamics is still observed in films which are in a

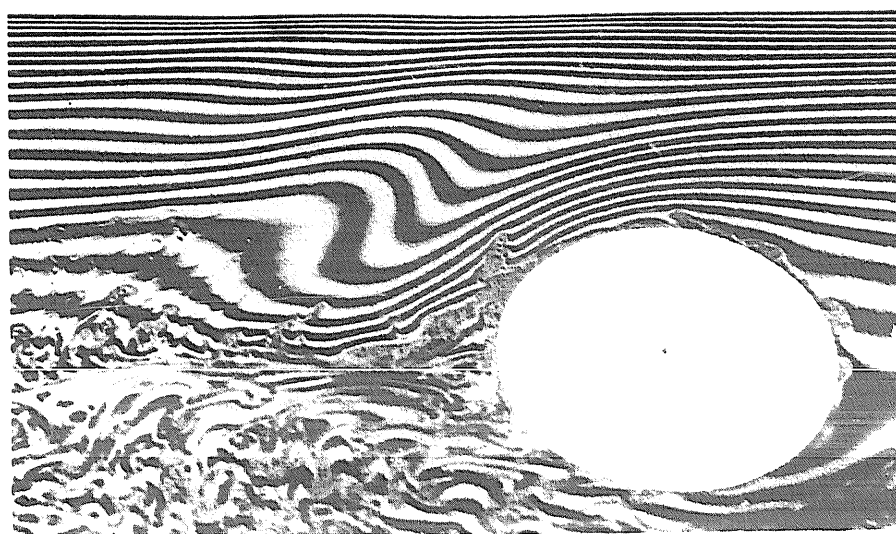


Fig. 13. The lee wave created by the motion of a large disk of aluminum paper moving (on the picture from left to right) in an inclined soap film.

Gibbs equilibrium. (If the hypothesis  $c_0 = \text{const.}$  (eq. (5)) is met, see note added in proof.)

## 7. Conclusion

We have presented very briefly several experiments aiming at the exploration of the dynamical properties of soap films. Though more work is still needed, we established some general characteristics.

– The physical properties of soap films are well known. We recalled classical results about their thermodynamics. The main asset is the chemical equilibrium between the soap molecules at the surfaces and the molecules of the interstitial fluid. Depending on the considered time scale of the film motions, the chemical equilibrium has time to establish itself or not. Therefore soap films have two elastic constants. On long time scales it has a Gibbs elasticity, and the fast response of the film is characterized by the Marangoni elasticity.

The Gibbs elasticity gives its quasi static state to a film. In the gravity field vertical films reach a quasi equilibrium where their two-dimensional thickness profiles are similar to the vertical density profile of the earth atmosphere. We have shown that such a quasi equilibrium is also reached when a film is set into a steady motion by a two-dimensional air flow. The film then reaches a thickness profile which provides an accurate visualization of the flow.

The Marangoni elasticity  $E_M$  characterises the dynamical response of the film. Our experiments are coherent with a film elasticity of this type on time scales up to the order of a second.

On short time scales each element of the film moves as whole so that the film can be considered as a two-dimensional fluid with a local density proportional to its thickness. We have written the equations of motion of a film where a surface tension term replaces the usual pressure term. Our experiments show that quasi two-dimensional turbulent flows are obtained in horizontal films. The film can be considered as incompressible whenever

the motions have velocities small compared to the velocity of its elastic waves (which are the equivalent of sound waves in gases). The main divergence from two dimensionality is due to the effect of air friction which damps the motion on all scales.

We showed that in a film set vertically buoyancy experiments could be performed. The motion of rising bubbles confirms that in the film at rest, surface tension gradient has the role of the hydrostatic pressure in normal fluids.

In the two-dimensional analogy the film's density is proportional to its thickness; a vertical film is from this point of view a strongly stratified fluid in which internal waves are observed.

## Acknowledgements

Our particular gratitude goes to H. Thomé with whom the experiments described therein were set. During periods of probation several students, M. Airiau, F. Darrigade, N. Gerard and D. Morel, were associated with the experiments. Joel Sommeria indicated to us the treatment of air friction by Landau and Lifshitz. We are grateful to Dr. K.J. Mysels for a very useful critical comment on the draft of this article.

## Note added in proof

The analysis carried out in the present article relies on the assumption that the overall soap concentration of a film element is the same everywhere in the film:

$$c_0 = c_1 + 2\Gamma_1 = \text{const.}$$

This hypothesis, used previously by Rusanov and Krotov [5], is necessary to carry out the calculation of the equilibrium profile of the film as well as the equations of its dynamics. However it is not obviously valid. The initial stretching of the film out of the bulk solution is not a well-controlled

process. If this stretching has been fast, the Gibbs equilibrium has not been maintained everywhere, and this could lead to films with regions of uneven soap concentration  $c_0$ . The surface of the film being large, the diffusive relaxation of these unevennesses in concentration would be very slow. The whole analysis of the initial equilibrium would then be upset and a correlation would appear between the thickness of a region and its soap concentration. The film would then be similar to a concentration stratified fluid. The existence of lee waves would then be linked to this characteristics. These waves corresponding now to the advection of regions of different chemical composition, it would no longer be necessary to explain their observation to assume a long typical time constant for the settling of the Gibbs equilibrium.

## References

- [1] J. Plateau, *Statique Expérimentale et Théorique des Liquides Soumis aux Seules Forces Moléculaires* (Gauthier-Villars, Paris, 1873).
- [2] J.W. Gibbs, *The Collected Works* (Longmans Green, New York, 1931).
- [3] C.V. Boys, *Soap Bubbles and the Forces Which Mould Them* (Society for Promoting Christian Knowledge, London, 1890 and Anchor Books, New York, 1959).
- [4] K.J. Mysels, K. Shinoda and S. Frankel, *Soap Films, Studies of Their Thinning* (Pergamon, New York, 1959).
- [5] A.I. Rusanov and V.V. Krotov, *Progr. Surf. Membrane Sci.* 13 (1979) 415.
- [6] Y. Couder, *J. Phys. Lett.* 42 (1981) 429.
- [7] M. Rabaud and Y. Couder, *J. Fluid Mech.* 136 (1983) 291.
- [8] Y. Couder, *J. Phys. Lett.* 45 (1984) 353.
- [9] Y. Couder, C. Basdevant and H. Thomé, *C. R. Acad. Sci. Paris* 299 (1984) 89.
- [10] C. Basdevant, Y. Couder and R. Sadourny, in: *Macroscopic Modelling of Turbulent Flows*, Lecture Notes in Physics 230 (Springer, Berlin, 1984).
- [11] J.M. Chomaz, M. Rabaud, C. Basdevant and Y. Couder, *J. Fluid Mech.* 187 (1988) 115.
- [12] Y. Couder and C. Basdevant, *J. Fluid Mech.* 173 (1986) 225.
- [13] M. Gharib and P. Derango, these Proceedings, *Physica D* 37 (1989) 406.
- [14] K.J. Mysels, M.L. Cox and J.D. Skewis, *J. Phys. Chem.* 65 (1961) 1107.
- [15] J. Lucassen and E.H. Lucassen-Reynders, *J. Colloid and Interface Sci.* 25 (1967) 496.
- [16] A. Prins, C. Arcuri and M. Van den Tempel, *J. Colloid and Interface Sci.* 24 (1967) 84.
- [17] G.I. Taylor, *Proc. R. Soc. London A* 253 (1959) 296.
- [18] J. Lucassen, M. Van den Tempel, A. Vrij and F. Hesselink, *Proc. K. Ned. Akad. Wetensch. B* 73 (2) (1970) 109, 124.
- [19] J.A. Kitchener and G.F. Cooper, *Quart Rev.* 1 (1959) 71.
- [20] S. Taneda, *J. Phys. Soc. Japan* 14 (1959) 843.
- [21] H. Aref and E.D. Siggia, *J. Fluid Mech.* 109 (1981) 435.
- [22] G.K. Batchelor, *Phys. Fluids* (suppl. II) 12 (1969) 233.
- [23] L.D. Landau and E.M. Lifshitz, *Fluid Mechanics* (Pergamon, New York, 1959), p. 149.
- [24] J.F. Harper, *Adv. Appl. Mech.* 12 (1972) 59.
- [25] P.P. Wegener and J.Y. Parlange, *Ann. Rev. Fluid Mech.* 5 (1973) 79.
- [26] R. Clift, J.R. Grace and M.E. Weber, *Bubbles, Drops and Particles* (Academic Press, New York, 1978).
- [27] D. Bhaga and M.E. Weber, *J. Fluid Mech.* 105 (1981) 61.
- [28] J.K. Walters and J.F. Davidson, *J. Fluid Mech.* 12 (1962) 408.
- [29] R. Collins, *J. Fluid Mech.* 22 (1965) 763; *Chem. Eng. Sci.* 20 (1965) 851.
- [30] J.R. Grace and D. Harrison, *Chem. Eng. Sci.* 22 (1967) 1337.
- [31] J.R. Crabtree and J. Brigwater, *Chem. Eng. Sci.* 22 (1967) 1517.
- [32] J.H. Hills, *J. Fluid Mech.* 68 (1975) 503.
- [33] T. Maxworthy, *J. Fluid Mech.* 173 (1988) 95.
- [34] R.M. Davies, and G.I. Taylor, *Proc. R. Soc. London A* 200 (1950) 375.
- [35] R.R. Long, *Tellus* 7 (1955) 342.
- [36] J.W. Miles and H.E. Huppert, *J. Fluid Mech.* 35 (1969) 4917.